On the Phase Noise Impact in Direct-Detection Optical OFDM Transmission

Wei-Ren Peng, Jason (Jyehong) Chen, and Sien Chi

***Abstract*—In this letter, we characterize the impact of laser phase noise (PN) in direct-detection optical orthogonal frequency-division multiplexing (OFDM) and emphasize its several differences from those in coherent optical OFDM. We also analyze the system performance in the presence of PN for various quadrature-amplitude-modulation formats and provide the bit-error-rate estimation method which can yield reliable results when the PN-induced optical signal-to-noise ratio penalty is lower than ∼2 dB.**

***Index Terms*—Direct detection, optical fiber communication, orthogonal frequency-division multiplexing (OFDM), phase noise (PN).**

I. Introduction

OPTICAL orthogonal frequency-division multiplexing (OFDM) has recently received much attention due to its flexible spectral efficiency and superior resilience against both fiber chromatic dispersion (CD) and polarization-mode dispersion (PMD) [1], [2]. To date, the OFDM systems could be implemented with either the coherent optical approach (CO-OFDM), or the direct-detection method (DDO-OFDM). DDO-OFDM, which uses the simpler hardware and the less-complex signal processing at a price of a worse receiving sensitivity when compared with CO-OFDM, would be an alternate format for next-generation metropolitan and long-haul terrestrial transmissions.

One claimed benefit of the DDO-OFDM systems is the relaxed requirement for the laser linewidth (LW): contrary to the high-cost external cavity laser (ECL) in CO-OFDM, a low-priced distributed-feedback (DFB) laser with a linewidth of several megahertz (MHz), in general, is considerably acceptable in DDO-OFDM because of the better phase coherency between the carrier and sideband [3]. However, due to fiber CD, the carrier and the sideband will gradually walk off with the increasing transmission distance and eventually will lose their phase coherency causing significant phase noise (PN) in detection. This phenomenon had first been identified in [4] with 12.5-Gb/s [32-quadrature-amplitude modulation (QAM)] data rate and 320-km fiber transmission. However, the PN characteristics in DDO-OFDM systems, which are found to be quite different from those in CO-OFDM, should be clarified in detail and emphasized from a view point of system design.

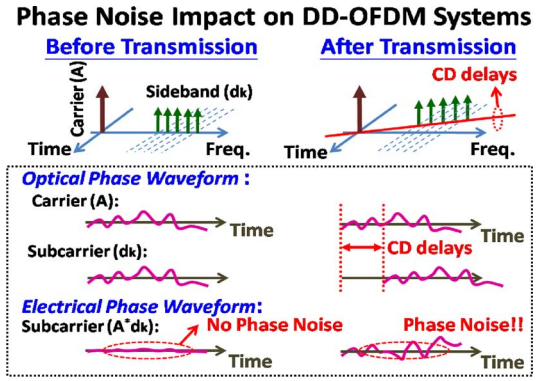

Fig. 1. Origin of PN in DDO-OFDM transmission.

In this letter, we find that the PN in DDO-OFDM has the following two significant differences from those in CO-OFDM: 1) the power and bandwidth of PN in DDO-OFDM are functions of both the subcarrier frequency and the transmission distance. Typically, a greater accumulated CD, i.e., the higher-frequency subcarrier with a longer transmission distance, would result in a larger PN power and a smaller PN bandwidth. Hence. the zeroth-order PN interference, previously the common phase error (CPE) [6], is no longer common to all subcarriers in DDO-OFDM. 2) The PN bandwidth, for most practical links, might range from hundred MHz to several gigahertz (GHz) which is independent of the laser LW. Such a broad spectrum will inevitably introduce significant intercarrier interference (ICI), making the PN compensator more difficult to design. On the other hand, in addition to the PN characterization, we also analyze the system performance with PN corruptions. The results show that, for a fixed data rate, even though the broader bandwidth of 4-QAM format would suffer the most accumulated CD, the larger symbol spacing could, however, provide a greater noise margin and make it most resilient against PN when compared with higher QAM formats. We also provide the bit-error-rate (BER) formula and, for the considered 4-, 16-, and 64-QAM formats, the estimated BERs are reliable provided the PN-induced optical signal-to-noise ratio (OSNR) penalty is $\leq\sim$2 dB.

II. PN Modeling and BER

The PN origin in a DDO-OFDM system can be realized via Fig. 1. Before transmission, the carrier and sideband will be coherent in phase such that there will be no PN after the photodiode and thus no impact on the received signal. After transmission, because of the relative walk-off, resulted from fiber CD, between the carrier and sideband, the PN will happen after the

Manuscript received November 27, 2009; revised February 01, 2010; accepted February 03, 2010. Date of publication February 22, 2010; date of current version April 09, 2010.

The authors are with Department of Photonics and Institute of Electro-Optical Engineering, National Chiao Tung University, HsinChu 300, Taiwan (e-mail: pwr.eo92g@nctu.edu.tw).

Color versions of one or more of the figures in this letter are available online at http://ieeexplore.ieee.org.

Digital Object Identifier 10.1109/LPT.2010.2042804

photodiode. Since the PN in DDO-OFDM comes from the interaction between the laser LW and CD, the power and bandwidth of PN will be shown to be functions of both the subcarrier frequency and the transmission distance.

To understand this direct-detection PN more thoroughly, we quantify the PN with the following parameters: the laser PN $\Phi(t)$ is modeled by the Wiener process [5] with a variance of $2\pi\gamma t$, where γ is the laser LW. Before transmission, the signal with laser PN can be modeled as $\{(A+\sum d_k e^{j2\pi f_k t})e^{j\Phi(t)}\}$, where j is the imaginary unit, A and d_k are the complex amplitudes of the carrier and kth data subcarrier [7], respectively, and f_k represents the frequency of the kth subcarrier. After transmission, the CD-induced walk-off will be involved into the signal model which now has a form of $\{Ae^{j\Phi(t)}+\sum d_k \exp[j2\pi f_k t + j\Phi(t+T_k)]\}$, where T_k is the relative time delay of the kth subcarrier with respect to the carrier and can be expressed as $T_k = (DL\lambda^2 f_k/c)$, of which c is the light speed in vacuum, D is the dispersion parameter, L is the fiber length, and λ is the operated wavelength. Then the kth subcarrier after the photodiode can be expressed as $Re\{A^*\sum d_k \exp[j2\pi f_k t + j\rho_k(t)]\}$, where $Re\{x\}$ takes the real part of x, the superscript "*" carries out the complex conjugation, and $\rho_k(t) = [\Phi(t+T_k)-\Phi(t)]$ stands for the converted electrical PN in DDO-OFDM systems [8]. After the fast Fourier transform (FFT) demodulator, the kth subcarrier signal can be represented as $R_k = d_k\psi_k(0)+\sum_{m\neq k} d_m\psi_m(k-m)$ [5], [6] with $\psi_k(p) = (1/N)\sum_n \exp[j2\pi pn/N + j\rho_k(n)]$, where N is the FFT size and $\rho_k(n)$ is the timely sampled function of $\rho_k(t)$. Note that the zeroth-order PN $\psi_k(0)$, conventionally CPE in CO-OFDM, is a function of the subcarrier index k (frequency) and, therefore, its value is no longer common to all the data subcarriers. Thus, we rename $\psi_k(0)$ simply as "phase rotation term (PRT)" here because typically it induces only the symbol rotation when PN is small [5], [6]. For DDO-OFDM, the received subcarrier signal R_k has a similar form as its wireless analogy [5], with the following extra assumptions: 1) PN of the signal–signal beat interference (SSBI) [7] is relatively small and can be omitted; 2) the PN-to-amplitude noise is negligible, which usually is true when the sideband is far from the carrier.

Now we obtain the electrical signal-to-noise ratio (ESNR) and BER by assuming that ICI from adjacent subcarriers are all independent and Gaussian-distributed [5]. The ESNR, without considering the PRT, $\psi_k(0)$, could be approximated as

$$\mathrm{ESNR}_k \approx \frac{1}{\sum\limits_{m\neq k}\psi_m(k-m)+\left(\frac{1}{\mathrm{ESNR}_{\mathrm{ASE},k}}\right)} \quad (1)$$

where $\mathrm{ESNR}_{\mathrm{ASE},k}$ is the ESNR of kth subcarrier with only the amplified spontaneous emission (ASE) noise [7]. The BER, with 4-QAM format, for each subcarrier should consider both the phase rotation of PRT and the Gaussian-noise terms of ASE and ICI, and can be obtained as follows [5]:

$$\mathrm{BER}_{k,4\mathrm{QAM}} \approx \frac{1}{4}\int_{-\infty}^{\infty}\begin{pmatrix}\mathrm{erfc}\left(\sqrt{\mathrm{ESNR}_k}\cos[\frac{\pi}{4}+\theta]\right)\\ +\mathrm{erfc}\left(\sqrt{\mathrm{ESNR}_k}\sin[\frac{\pi}{4}+\theta]\right)\end{pmatrix} f_k(\theta)d\theta \quad (2)$$

where θ is the random phase rotation and $f_k(\theta)$ is Gaussian distributed with a variance of $\psi_k(0)$. The system BER can then be obtained by taking the average of BER_k [7]. Notably, the BER with higher QAM formats can be easily derived in a similar manner [5].

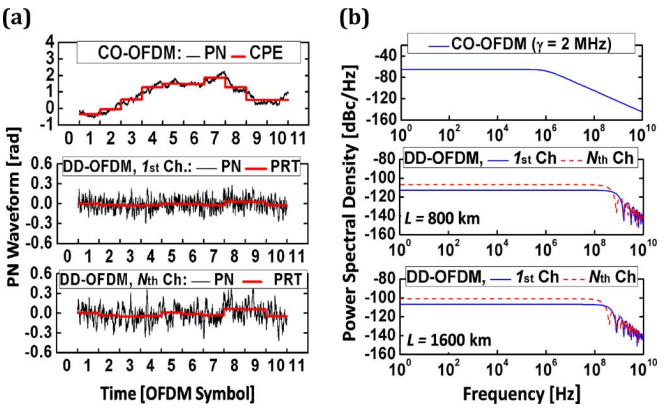

Fig. 2. (a) PN waveforms versus OFDM symbols for CO- and DDO-OFDM systems. (b) Power spectral density (PSD) of PN. Top: CO-OFDM. Center: DDO-OFDM with 800-km SSMF. Bottom: DDO-OFDM with 1600-km SSMF. $N = 160$.

III. Numerical Results and Discussion

In simulations, we consider the typical gapped-OFDM transmission [1] with 20-Gb/s data rate, 160 data subcarriers, 1024 FFT size, 20% cyclic prefix, 2-MHz laser LW, and 16-ps/(nm.km) dispersion parameter for transmission fiber. The second-order Gaussian optical filters are used with a 3-dB bandwidth equal to 1.2 × (signal bandwidth). In Figs. 2 and 3, we first compare the PN characteristics of the CO- and DDO-OFDM systems with 16-QAM format. In Fig. 2(a), we show the PN waveforms of $\Phi(t)$ and $\rho_k(t)$ for the CO- and DDO-OFDM systems, respectively, with 1600-km fiber transmission. For DDO-OFDM, we show the results of both the 1st and 160th subcarriers to emphasize the frequency dependency. The larger PN variance in CO-OFDM is observed because of the random walk nature of the Wiener process, which allows the phase to travel unlimitedly with increasing time. On the other hand, the PN power of DDO-OFDM will be constrained by its variance of $\sim 2\pi\gamma T_k$ and thus would not go unboundedly. Also, in DDO-OFDM, the PN power of 160th subcarrier is ∼twice as large as that of the first subcarrier due to the doubled accumulated CD. In Fig. 2(b), we show the PNs' PSD, which are analytically provided in [8], for both the CO- and DDO-OFDM systems. For DDO-OFDM, the results of the 1st and 160th subcarriers are shown with 800- and 1600-km fiber transmission. The one-sided 3-dB PN bandwidth of DDO-OFDM (∼174 MHz for 160th subcarrier with 1600-km transmission) is found to be much broader than that of CO-OFDM (∼1 MHz), and be a function of both the subcarrier frequency and the transmission distance. Typically, a higher subcarrier frequency (i.e., 160th subcarrier) with a longer transmission distance (i.e.,1600 km) would result in a larger PN power and a narrower PN bandwidth. In Fig. 3, we further show the received constellations for CO- and DDO-OFDM systems with 1600-km transmission. For CO-OFDM, the CPE has a relatively larger power than ICI and would strongly rotate the subcarrier phase so that the CPE compensator is a must at the receiver [6]; while for DDO-OFDM, although the PRT would similarly degrade the signal by introducing some phase deviations, due to its broader PN bandwidth, the ICI shows a

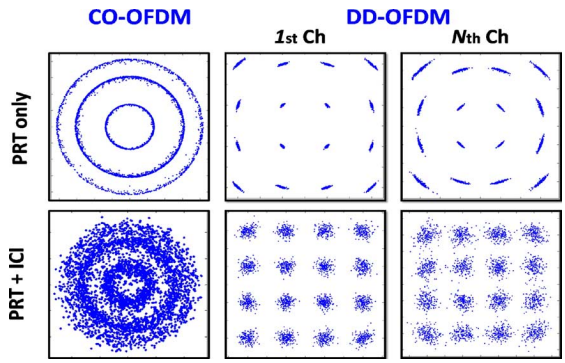

Fig. 3. Effects of PRT and ICI on 16-QAM format in both CO- and DDO-OFDM systems. $\gamma = 2$ MHz, $N = 160$, $L = 1600$ km.

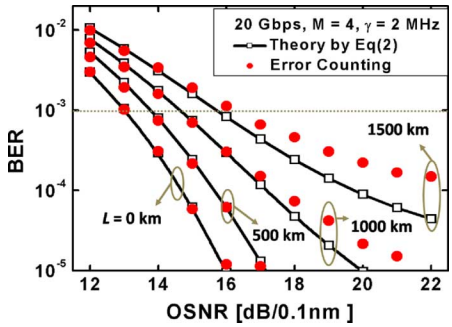

Fig. 4. BER versus OSNR with different transmission distances.

relatively larger power and has a more significant impact on the signal quality.

In Fig. 4, the BER performance in terms of OSNR, obtained by the error counting (EC) method, are shown for DDO-OFDM systems in the presence of PN. The 4-QAM format is utilized in systems with different transmission lengths of 0, 500, 1000, and 1500 km. The theoretical estimations of (2) are also shown for comparisons. The OSNR penalty is found to be enlarged with an increasing fiber length L, and the BER floor could be found when L is $\geq$1000 km. The estimations by (2) are found to match the EC results only when the PN power is relatively smaller, i.e., under the conditions of either a higher OSNR value or a shorter transmission distance. When the PN power becomes larger, (2) will fail to yield an accurate BER. This inaccuracy could be attributed to the pattern effect of the subcarrier signal [9], which needs exhausted and almost prohibitive computations and thus is not considered in (2).

In Fig. 5, we investigate the OSNR penalty versus transmission distance with diverse QAMs. Again both the EC results and the estimations (2) are compared. First of all, from the EC results, the maximum distance of 4-, 16- and 64-QAM formats with 2-dB OSNR penalty are found to be $\sim$1200, 600, and 300 km, respectively, which demonstrates that the 4-QAM format, which exhibits a larger noise margin with the sacrifice in spectral efficiency, has a better PN tolerance achieving a longer transmission distance. Note that here the different QAMs are switched with a fixed data subcarrier number, while similar results will be obtained if the QAMs are switched with a fixed OFDM symbol duration. Then, from the theoretical estimations, we found the estimations by (2) would deviate from the exact EC results when the OSNR penalty is

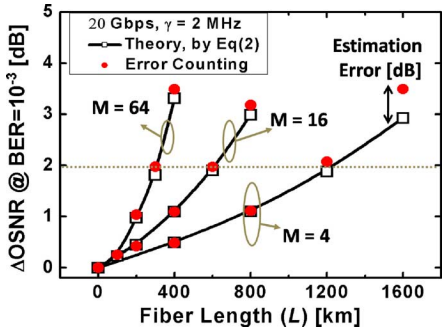

Fig. 5. OSNR penalty versus fiber length for 4-, 16-, and 64-QAMs.

large. If the maximum estimation error, which is defined as, given a fiber distance L, the penalty difference between the EC results and the estimations by (2), is allowed to be 0.2 dB, we found that (2) can offer an acceptable estimation for both 16- and 64-QAM formats when the OSNR penalty is up to 3 dB; while for the 4-QAM format which suffers stronger PN, (2) can still yield a reliable estimation when the OSNR penalty is $\leq\sim$2 dB. This demonstrates that (2) can reliably estimate the OSNR penalty when the OSNR penalty is $\leq\sim$2 dB for all the considered QAM formats.

In conclusion, based on the discussions above, the previous CPE compensator [6], which ignores the ICI effect, would inefficiently assist in recovering the PN-corrupted signals in DDO-OFDM. On the other hand, the broader PN bandwidth in DDO-OFDM would make the RF-pilot compensator [2], [5], which needs a frequency guard band with a width of approximately the PN bandwidth, a less spectrally efficient method. Therefore, the PN in DDO-OFDM might motivate a new PN solution for high-capacity and long-distance transmission that uses DFB lasers.

REFERENCES

[1] B. J. C. Schmidt, A. J. Lowery, and J. Armstrong, "Experimental demonstrations of electronic dispersion compensation for long-haul transmission using direct-detection optical OFDM," *J. Lightw. Technol.*, vol. 26, no. 1, pp. 196–203, Jan. 1, 2008.

[2] S. L. Jansen, I. Morita, T. C. W. Schenk, N. Takeda, and H. Tanaka, "Coherent optical 25.8 Gb/s OFDM transmission over 4160-km SSMF," *J. Lightw. Technol.*, vol. 26, no. 1, pp. 6–15, Jan. 1, 2008.

[3] D. Qian, J. Yu, J. Hu, L. Zong, L. Xu, and T. Wang, "10 Gb/s WDM-SSB-OFDM transmission over 1000 km SSMF using conventional DFB lasers and direct-detection," *Electron. Lett.*, vol. 44, no. 3, pp. 223–225, Jan. 2008.

[4] Z. Zan, M. Premaratne, and A. J. Lowery, "Laser RIN and linewidth requirements for direct detection optical OFDM," in *Proc. CLEO'08*, San Jose, Paper CWN2.

[5] M. S. El-Tanany, Y. Wu, and L. Hazy, "Analytical modeling and simulation of phase noise interference in OFDM-based digital television terrestrial broadcasting systems," *IEEE Trans. Broadcasting*, vol. 47, no. 1, pp. 20–31, Mar. 2001.

[6] X. Yi, W. Shieh, and Y. Ma, "Phase noise effects on high spectral efficiency coherent optical OFDM systems," *J. Lightw. Technol.*, vol. 26, no. 10, pp. 1309–1316, May 15, 2008.

[7] W.-R. Peng, K.-M. Feng, A. E. Willner, and S. Chi, "Estimation of the bit error rate for direct-detected OFDM signals with optically pre-amplified receivers," *J. Lightw. Technol.*, vol. 27, no. 10, pp. 1340–1346, May 15, 2009.

[8] G. Qi, J. Yao, J. Seregelyi, S. Paquet, C. Belisle, X. Zhang, K. Wu, and R. Kashyap, "Phase-noise analysis of optically generated millimeter-wave signals with external optical modulation techniques," *J. Lightw. Technol.*, vol. 24, no. 12, pp. 4861–4875, Dec. 2006.

[9] R. Corvaja and S. Puolin, "Phase noise spectral limits in OFDM systems," *Wireless Personal Commun.*, vol. 36, pp. 229–244, 2006.